Subcellular Electrical Stimulation of Neurons Enhances the Myelination of Axons by Oligodendrocytes.

Hae Ung Lee[1]*, Agata Blasiak[1]*, Devansh R. Agarwal[1], John S. Ho[1,2], Nitish Thakor[1,3], In Hong Yang[1,3,]

[1]Singapore Institute for Neurotechnology, National University of Singapore, Singapore.

[2]Department of Electrical and Computer Engineering, National University of Singapore.

[3]Department of Biomedical Engineering, School of Medicine, Johns Hopkins University, Baltimore, USA.

*These authors share first authorship

Correspondence: In Hong Yang (**iyang3@jhmi.edu, lsiyang@nus.edu.sg**)

Abstract (200 words)

Myelin formation has been identified as a modulator of neural plasticity. New tools are required to investigate the mechanisms by which environmental inputs and neural activity regulate myelination patterns. In this study, we demonstrate a microfluidic compartmentalized culture system with integrated electrical stimulation capabilities that can induce neuron activity by whole cell and focal stimulation. A set of electric field simulations was performed to confirm spatial restriction of the electrical input in the compartmentalized culture system. We further demonstrate that electrode localization is a key consideration for generating uniform neuron stimulation within the compartments. Using our system we tested the effects of subcellular activation of neural activity on distal axon myelination with oligodendrocytes. An isolated stimulation of cell bodies and proximal axons had the same effect as an isolated stimulation of distal axons co-cultured with oligodendrocytes, and the two modes were non-different than whole cell stimulation. Our platform enabled the demonstration that electrical stimulation enhances oligodendrocyte maturation and myelin formation independent of the input localization.

Introduction

Myelin sheaths play pivotal roles as an axon isolator and an conductor of electrical signals in nerve system. In the recent years, the function of myelination has been identified to not only potentiate conduction of neural signals but to affect neural function and plasticity as well (reviewed in [1, 2]). The *in vivo* evidences of such myelin-based plasticity mechanisms were demonstrated in behavioral studies in both juvenile and adult mice. Social isolation of two-week-old pups resulted in thinner and lower number of myelin sheaths, which in turn affected social interactions and working memory [3]. Similarly, socially isolated adult mice demonstrated thinner myelin sheaths, lower level of gene expression specific to myelination, and behavioral deficits. The two latter effects were reversed in 4 weeks after reintroducing social stimuli, emphasizing the remodeling ability of myelination process [4]. Finally, myelin-forming oligodendrocyte (OLs) generation was shown to correlate with motor learning – teaching a mouse a complex running task increased OLs formation, while a knockout animal with reduced oligodendrogenesis demonstrated impaired learning performance [5]. Those observations are indicative of a link between environmental stimuli, central nervous system (CNS) plasticity and myelination.

On a cellular level, axon conductivity can be dynamically affected by the changes in a structure of myelin sheath, including modulation of its thickness, length, and axon coverage [2, 6]. In turn, it has been shown that axon activity itself, although not prerequisite for OLs wrapping process [7, 8], supports oligodendrogenesis [9], induces *de novo* myelin formation [10, 11] and increases the thickness of the sheaths [12]. As the environmental stimuli are converted into neuronal circuit activity patterns, the neural activity-dependent myelination may play a crucial role in myelin-based regulation of CNS cognitive activity and learning. Those mechanisms remain unclear.

A common system for investigating myelination mechanisms is mixed neuron/glia co-culture in a dish or multi-well plate. Although easy to manipulate, these systems hinder identification of the mediator for signaling molecules, whether oligodendrocytes or neurons. Furthermore, they do not recapitulate

the *in vivo* scenario, where neuronal cell bodies and majority of myelinating axons in a brain are spatially concentrated in different areas. Compartmentalized co-culture systems have been used to separate neuronal cell bodies in space and milieu, facilitating exclusive interaction of oligodendrocytes with distal axons [13, 14]. These models enable dissection of subcellular myelination mechanisms, which are important considering a focal scope of neuron activity stimulation with e.g., optogenetic technique or electrodes. Compartmentalized platforms have been successfully integrated with electrical stimulation for studying activity dependent myelination [11, 15, 16]. However, the effects of spatially restricted neural activity input associated with myelination have not been explored.

In this study we describe a compartmentalized platform for whole cell and subcellular electrical stimulation of neurons, cell bodies and axons. We performed a set of simulations to understand the characteristics of the electric field and ensure restricted stimulation input. The simulations further demonstrate the importance of the compartment sizes and electrode positions within them. Finally, we show that subcellular stimulation enhances distal axon myelination on the same level as whole cell stimulation.

Material and Methods

Microfluidic Platform

The fabrication process of the two-chamber microfluidic platforms connected by a set of parallel microchannels (10-μm-wide, 2.5-μm-high and 500-μm-long) followed a previously published protocol [16-18]. Briefly, the masters were fabricated by standard photolithography, and negative photoresist SU8 was used as the master layer for silicon (Si) wafer. The devices were prepared in polydimethylsiloxane (PDMS, Dow Corning Sylgard 184 Silicone elastomer) by mixing a base with a curing agent in 10:1 ratio, pouring on the Si wafer, degassing it in a vacuum for 1hr and curing at 70 °C for 2 hours. After curing, the chambers were punched out with rectangular shaped punches prepared by reshaping circular Ø8 mm biopsy punches (Ted Pella). The PDMS pads were bonded to

glass coverslips (thickness 1, Menzel Glaser) by oxygen plasma treatment (Femto Science) and were sterilized by autoclaving (120°C for 30 min).

Electric Field Simulations

Electric field simulations were performed using the finite element method (CST Computer Simulation Technology). Electrodes were modelled using Pt cylinders of 0.25mm radius. For the simulations, the compartments were assumed to be filled in with saline solution with dielectric constant $\varepsilon_r = 80$ [19, 20]. The dielectric constant of the surrounding material was assumed $\varepsilon_r = 3$, which is a dielectric constant for PDMS [21]. The polarity of the electrodes was assumed constant. The electric field coverage area was calculated using MATLAB (Mathworks) based on the maximum field magnitude in each configuration.

Cell Culture

Dorsal root ganglion (DRG) neurons were collected from E13 ICR mice embryos as described previously [15]. Dissected DRGs were digested in trypsin (Life Technologies), followed by trituration. The sterile PDMS devices were coated with 0.1 mg/ml poly-D-lysine (PDL) and 5 µg/mL Laminin (Life Technologies) by overnight incubation in 4°C. Dissociated cells (approximately 160,000 cells/cm^2) were seeded in the somatic chamber of the devices in Neurobasal media (Gibco) supplemented with B27 (Gibco), GlutaMAX-1 (Life Technologies), and nerve growth factor (NGF, 20 ng/mL; R&D systems). The cultures were maintained *via* half-volume media changes every 2–3 days. Flurodeoxyuridin (FudR, 13 µg/mL; Sigma) and Uridine (33 µg/mL; Sigma) were added for 4–6 days to eliminate non-neuronal populations.

Oligodendrocyte precursor cells (OPCs) were prepared from the brains of postnatal day 1 mice pups. The brain was dissected to isolate the two cortices. The meninges of the cortices were carefully removed and the cortices were minced into small pieces before dissociation with Neural Tissue Dissociation Kits (P) (Miltenyi Biotec) followed by processing with gentleMACS^{TM} Dissociator (Miltenyi Biotec). Dissociated brain cells were tagged with anti-O4 microbeads (Miltenyi Biotec) and O4-positive OPCs were purified by magnetic separation system (MACS Separator; Miltenyi Biotec).

The purity of separated OPCs was verified by anti-O4-PE (Miltenyi Biotec), and was found to be 85-90%. Newly purified OPCs were plated (100,000 cells/cm^2) in an axonal chamber of 10 day old DRG culture. DMEM containing Holo-transferrin (49.5 mg/L; Sigma), Bovine insulin (5 mg/L), progesterone (0.06 mg/L), putrescine (16.1mg/L), selenite (0.05 mg/L)], and 0.5% fetal bovine serum (FBS) were used to maintain DRG/OPCs co-cultures. Co-cultures were maintained in the absence of added growth factors for a total of 14 days (10 day old DRGs are NGF-independent) with half-volume media changes every 2–3 days.

Electrical Stimulation

Neuronal activity was induced using 0.2 ms biphasic pulses at 10 Hz. Pulse trains were applied for 0.5 s during every 2 s. The platinum electrodes that extended down into the platform were connected to a constant voltage power supply of 3 V. The stimulation pulses were applied for 1 h daily using a MultiStim System D-330 stimulator (Digitimer). The cultures remained in the incubator (37 °C, 5% CO_2) during the stimulation. The platforms containing electrodes that were not connected to the power source served as unstimulated controls.

Immunostaining and Imaging

Co-cultures were fixed with 4% paraformaldehyde by incubation for 30 min at room temperature and subsequent rinsing with Dulbecco's phosphate buffered saline (DPBS, Gibco). Cells were treated for 30 min in room temperature with a blocking buffer containing 5% goat serum (Sigma) and 0.1% Triton (Sigma) in DPBS. Subsequently samples were incubated with primary antibodies diluted in blocking buffer overnight at 4°C. Primary antibodies included mouse anti-O4 (Millipore, 1:500), mouse anti-myelin basic protein (MBP; Millipore, 1:1000), mouse or rabbit anti-neurofilament (Cell Signaling, 1:500), and rabbit anti-CNPase (Cell Signaling, 1:1000). Cells were washed twice with DPBS and incubated with two of the following secondary antibodies diluted in blocking buffer for 30 min at room temperature (RT): Alexa488 goat anti-mouse (1:200; Life Technologies), Alexa488 anti-rabbit (1:200; Molecular Probes), Alexa594 goat anti-rabbit (1:200; Life Technologies), Alexa594 anti-mouse(1:200; Molecular Probes). Finally, cells were washed with DPBS and deionized water,

and mounted in antifade solution (prolong gold antifade; Life Technologies). Imaging was performed using an inverted, confocal microscope (Zeiss). The whole area of the axonal compartment that contained axons was imaged in FITC, and TRITC channels. The numbers of cell with high O4, MBP and CNPase signals were counted manually. Similar, the myelin fragments with MBP and neurofilament signal colocalization were counted manually. Each experimental group contained at least 3 independent cultures.

Statistical Analysis

Statistical comparisons were performed by one-way ANOVA with Bonferroni-Holm post-hoc testing. A two-tailed Student's t-test was performed between groups in a pair- wise fashion with statistical significance at $P < 0.05$.

Results and Discussion

Whole Cell and Subcellular Stimulation with Electric Field - Simulations

We aimed to achieve subcellular electrical stimulation (ESTIM) by exploiting the compartmentalized neuon/glia co-culture. To understand the characteristics of the electric field in the compartmentalized system, we performed a set of simulations for different sizes of compartments and different configurations of the platinum electrodes. Our microfluidic platform contained two compartments, somatic and axonal, connected with 2.5-µm-high, 10-µm-wide, and 500-µm-long microchannels. The compartments were open to the air to provide an access, ease of manipulation, and buffering capacity. The dimensions of the compartments were: 7 mm length, 4 mm width and 7 mm height. The volume of each compartment was approximately 200 µL to limit evaporation and provide sufficient media for cell culture.

Our compartmentalized culture system was integrated with electrical stimulation (Fig. 1A and 1B). To better understand the electric field characteristics, we perform a set of finite element simulations for different configuration of electrodes. When the electrodes were placed in the mid-width of each compartment the field magnitude in the middle between the electrodes was 20.3 % of the maximum observed at the electrodes (Fig. 1C and 1E). 47.72 % of the compartments surface area was exposed

to the effective field, defined as the region with electric field magnitude within 10 % of the maximum. When the electrodes were shifted to the top of the device (Fig 1D) the effective field covered only 28.89 % of the compartments.

We then simulated the electric field when the electrodes were positioned diagonally within axonal compartment (Fig.1E) and in two different compartments (Fig. 1F). The first configuration generated electric fields predominantly in the axonal compartment; however, 9.48 % of the somatic compartment was exposed to the effective field (Fig. 1J). Placing the electrodes in the diagonal corners of two different compartments limited the magnitude of the field between them to 6.12 % of the maximum and only 23.03 % area of the compartments was covered by the effective field. Finally, we simulated the electric field when the two electrodes were located 4 mm apart in the middle of the somatic (Fig. 1G) or axonal (Fig. 1H) compartments. In both scenarios, the effective field was fully restricted to the compartment where the electrodes were placed and covered 93.54 % of the area of its area. The field magnitude in the middle between the electrodes was 22.76 % of the maximum (Fig. 1I).
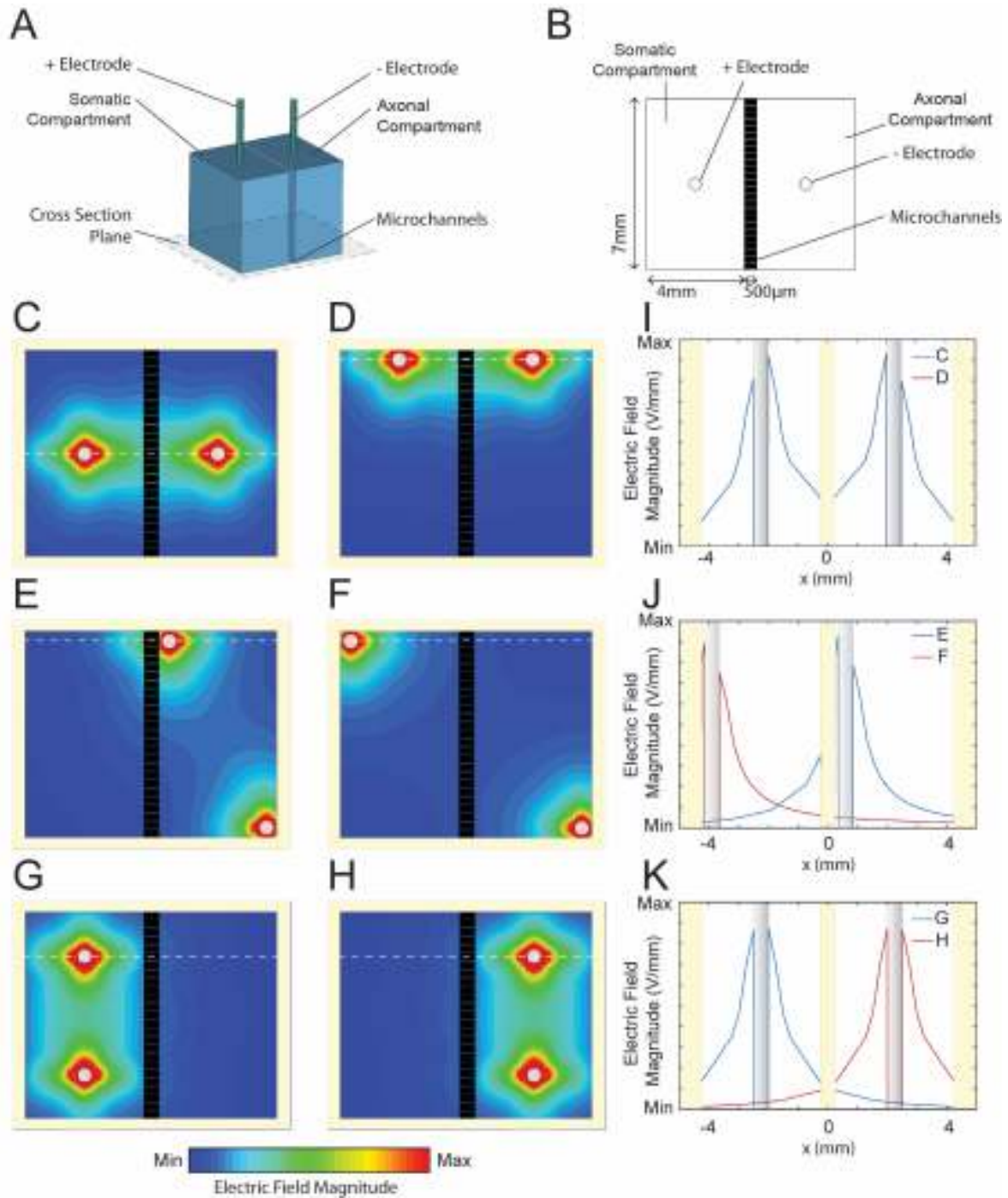
Figure 1. Electric field strength within the compartments. *A.* Schematic of the simulation model. *B.* Cross-section of model along indicated plane. **C-H**. Contour map of electric field magnitude within compartments for different electrode configurations. *I-K* Profile of electric field magnitude along dashed lines in (*C-H*) indicates strength of electric field across the two wells.

The results of our simulations indicate that the localization of electrodes is one of the key parameters for electrical stimulations in a compartmentalized culture system. As neurons require stimulation above a threshold to induce their action potential [22], the irregularity and the spatial restriction of the

electric field has several practical consequences to be considered when designing the setup: (1) the simultaneous stimulation of somatic and axonal compartments is the most efficient when the electrodes are located in the middle of the compartments; (2) the external electrical input can be spatially restricted to one compartment only if the electrodes are placed in the middle of the compartment, (3) however, the diagonal localization of the electrodes in the same compartment will result in partial stimulation of the opposite compartment; (4) the localization of the electrodes in the far corners of the two compartments is the least effective stimulation mode.

Intrigued by the spatial restriction of the electric field in our system, we performed another set of simulations to test how the dimensions of the compartments affect the coverage with the effective electric field. This information is important considering that commercially available compartmentalized systems for neuron culture can have a wide range of compartments dimensions. The length of somatic and axonal compartments in our simulation was increased to 15 mm (Fig. 2A and B) and three electrode placements were considered for simultaneous stimulation of both compartments. The mid-length and mid-width electrode configuration (Fig. 2C) provided effective field coverage of only 19.95 % of the compartments surface area. The minimum field magnitude between the electrodes was 14.54 % of the maximum. Moving the electrodes diagonally (Fig. 2D) increased the effective field coverage to 22.82% but decreased the minimum field magnitude between the electrodes to 8.11% of the maximum. Finally, placing the electrodes in the far corners of the device (Fig. 2E) minimized the compartments surface area exposed to the effective field to 5.91% and decreased the minimum field magnitude between the electrodes to 2.49%. These results further emphasize the need for careful consideration of the electrical stimulation system, especially when using commercially available neuron compartmentalized cultures.

 Compartmentalized culture integrated with the platinum rods as electrodes is an easy and versatile system for electrical stimulation [23]. If the homogeneity of the electric field is a crucial element of the experimental design other methods should be considered, e,g, microelectrode arrays for electrical stimulation [24].
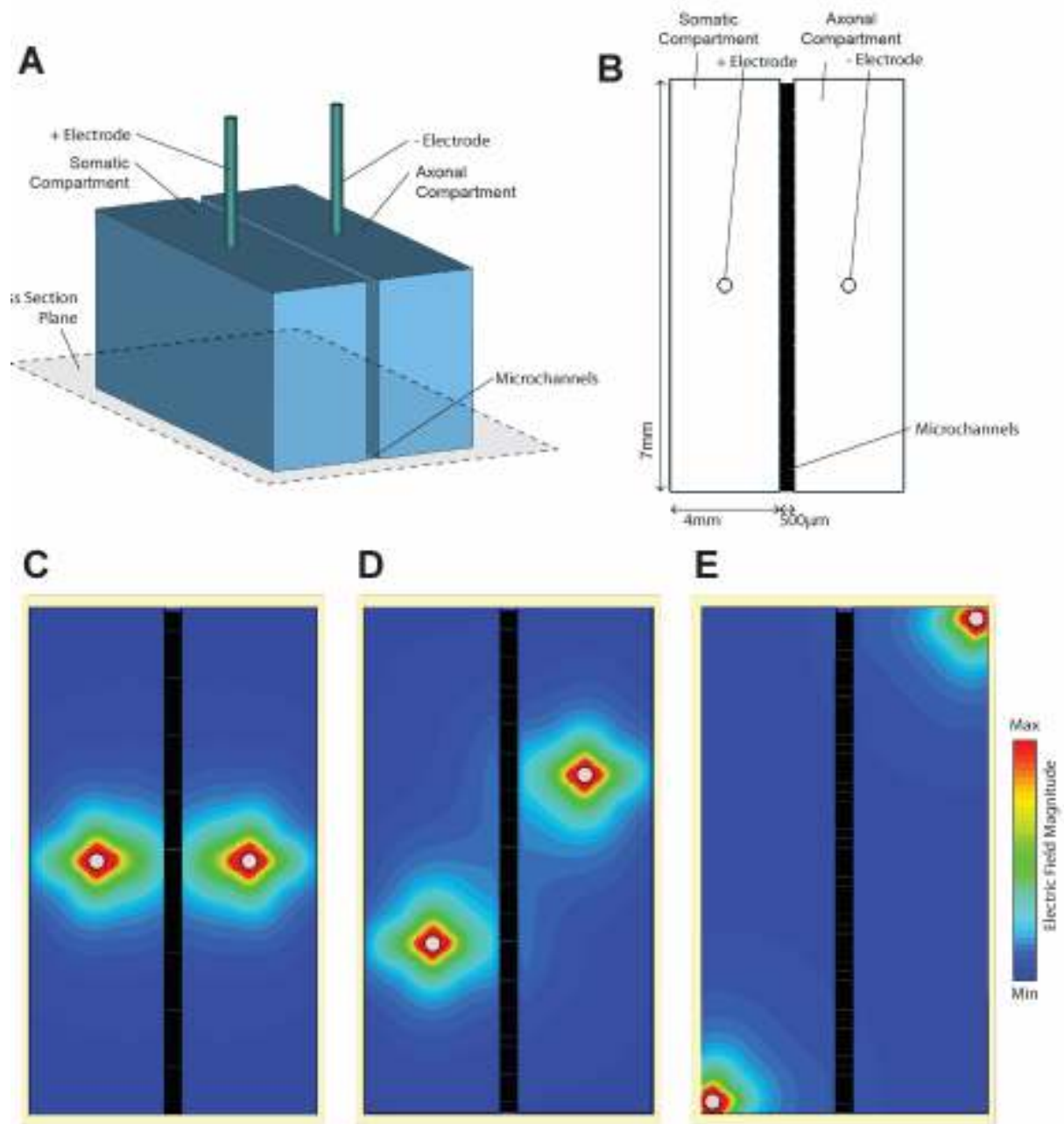
Figure 2. Electric field strength within the long compartments. *A*. Schematic of the simulation model. *B*. Cross-section of model along indicated plane. **C-E**. Contour map of electric field magnitude within compartments for different electrode configurations.

Integrated Compartmentalized Co-culture System with Subcellular ESTIM

Dorsal root ganglion neurons (DRGs) were obtained from E13 ICR mice embryos and plated in the somatic compartment of the bicompartmental device. Cell bodies extended neurites, which extensively elongated and by 4 day *in vitro* (DIV) crossed to the axonal compartment. At 10 DIV high number of axonal processes was present in the axonal compartment and this is when oligodendrocyte precursor cells (OPCs) collected from postnatal day 1 mice pups were plated in that compartment. The set of parallel microchannels connecting somatic and axonal compartment allowed axons, but prohibited cell bodies from passing, providing spatial isolation of neuronal cell bodies and distal axons with OPCs. Accordingly, no OPCs were observed in the somatic compartment, confirming the spatial isolation and exclusive contact between OPCs and distal axons. Good viability of the cells was sustained for at least 14 days in co-culture. After 3 days OPCs started developing processes typical for oligodendrocytes (OLs) indicating their differentiation. In comparison to cortical and hippocampal neurons, DRGs in *in vitro* culture demonstrate relatively little spontaneous action potentials and synchronization. This feature makes it easier to distinguish the effects of externally induced neuron activity over the effects of the inherent firing.

ESTIM was performed for 1h a day in DRG/OPC co-cultures starting on the day of OPCs plating. Three configurations of electrodes were used to induce neuronal activity: (1) WholeSTIM (Fig 1C): This configuration stimulated the cell bodies in the somatic compartment and distal axons with OPCs in the axonal compartment; (2) SomaSTIM (Fig 1G): This configuration induced neuronal activity of the cell bodies and proximal axons, while the myelination was assessed in the axonal compartment; (3) AxonSTIM (Fig 1H): This configuration stimulated the distal axons in the axonal compartment as well as oligodendrocytes (Fig 3A). The cells were stimulated with 10 Hz, 3 V-high, 0.5 ms-wide rectangular biphasic pulses forming trains that last for 0.5 s, repeated after 2 s for 1 hour a day. The stimulation parameters were the same for all the ESTIM modes and were previously used to study activity-dependent myelination (Fig 3B) [11, 15, 25]. The control culture contained electrodes not connected to the power source.
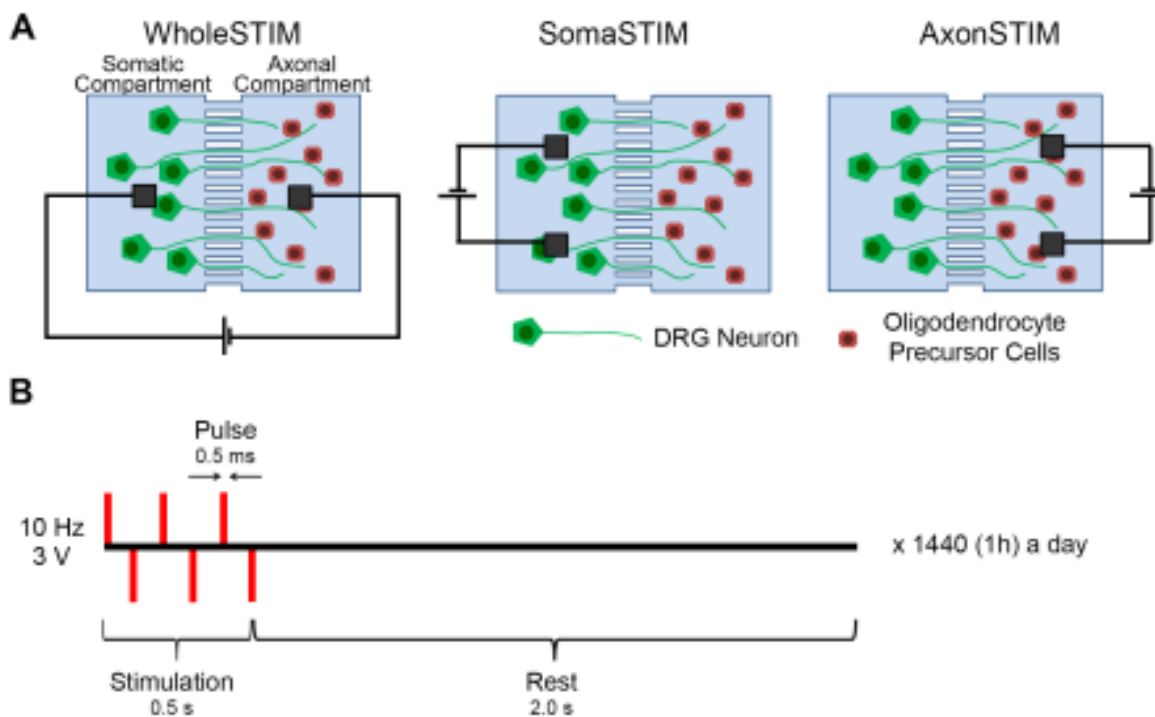
Figure 3. Integrated compartmentalized and electrical system for subcellular stimulation of neurons. *A.* Dorsal root ganglion neurons and oligodendrocyte precursor cells were cultured in microfluidics and electrically stimulated in three different modes of electrode configuration: whole cell stimulation (WholeSTIM), somatic compartment stimulation (SomaSTIM) and axonal compartment stimulation (AxonSTIM). *B.* The schematic of stimulation protocol.

Subcellular Specific ESTIM Promoted the Differentiation of Oligodendrocytes and Myelination.

To quantify the effects of ESTIM on axon myelination, we first tested if it enhanced OPCs differentiation into OLs that have a capability to wrap around the axons. We applied ESTIM in all three configurations, fixed the cells and stained for the differentiation markers. 1 day of ESTIM did not affect the number of premature OPCs as visualized with anti-O4 antibody [26] (Fig. 4A and 4E). However, after 3 days of ESTIM in all three electrode configuration, we observed a substantial shrinkage of the premature OPCs population. This decline was significantly more pronounced than the modest decrease observed in the control culture. These results suggest that the externally evoked neuron activity was not necessary for OPCs differentiation, but significantly enhanced the baseline

differentiation (Fig. 4F). Interestingly, no differences were detected in the results of ESTIM in three different electrodes configurations. We then aimed to test if the decrease in the number of premature OPCs was followed by the increase in the number of mature OLs. We fixed the cells after 7 days of the stimulation and stained glia cells against myelin basic protein (MBP) and 2',3'-Cyclic-nucleotide 3'-phosphodiesterase (CNPase) – the markers of mature OLs [26] (Fig. 4B and 4C). The numbers of MBP-positive and CNPase-positive cells were significantly higher after ESTIM than in the control cultures (Fig. 4G and 4H). Consistent with O4 staining results, no differences were detected in the effects of the electrode configurations. We aimed to test if the increased differentiation of OPCs into OLs resulted in increased myelination. We stimulated the co-cultures for 14 days, fixed and stained against MBP. We counted myelin fragments defined as fully overlapping neuronal processes with MBP-positive OLs structures (Fig. 4D). ESTIM significantly increase the number of myelin fragments compared to the control group (Fig. 4I). No differences were detected between the ESTIM modes. Taken together, our results strongly imply that ESTIM enhanced differentiation of premature, O4-positive OPCs into MBP-positive and CNPase-positive mature OLs and accordingly, increased the number of myelination events.
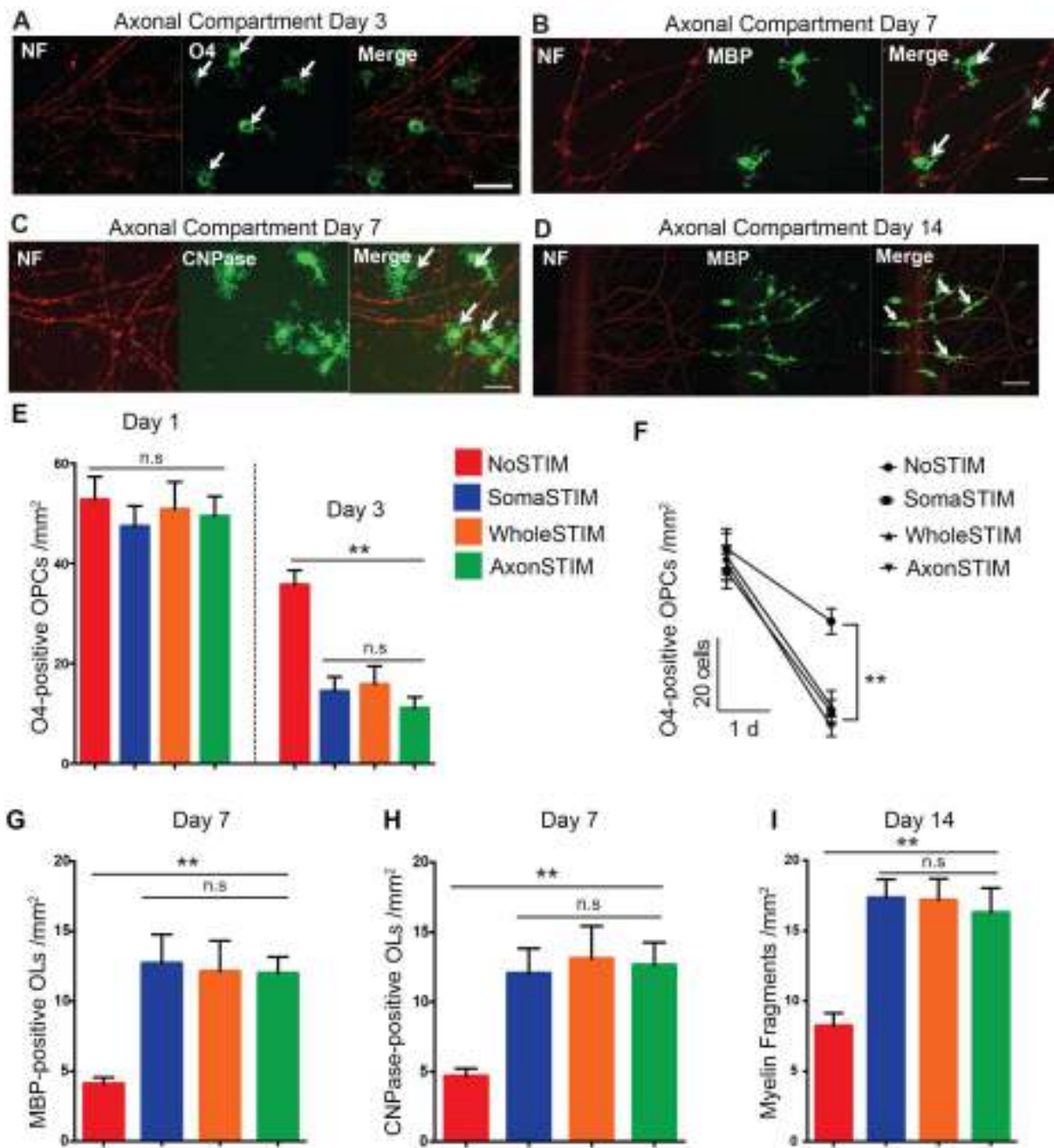
Figure 4. Whole cell and subcellular ESTIM enhances oligodendrocyte precursor cells (OPCs) differentiation into oligodendrocytes (OLs) and supports axon myelination. *A-D.* Representative images of axons in the axonal compartment stained against neurofilaments (NF, red) and OLs stained against a set of differentiation markers: *(A)* O4 signal (green) expressed by premature OPCs (white arrows) after 3 days of stimulation; *(B)* CNPase signal (green) expressed by mature OLs (white arrows) after 7 days of stimulation; *(C)* MBP signal (green) expressed by mature OLs (white arrows) after 7 days of stimulation; *(D)* MBP signal (green) expressed by mature OLs after 14 day of stimulation demonstrating formed myelin sheath fragments (white arrows). Scale bar (*A - D*): 50µm. *E.* ESTIM decreased the number of O4-positive OPCs after 3 days of stimulation. *F.* The number of

O4-positive OPCs decreased after 3 days in the control group outlining the baseline level of the differentiation. *G-H.* 7 days of ESTIM supported OLs maturation as indicated by the numbers of MBP-positive *(G)* and CNPase-positive *(H)* cells. *I.* 14 days of ESTIM increased the number of formed myelin fragments. The data are presented as mean ± s.e.m., **p<0.001.

The increase in the OLs maturation and myelin sheath formation after whole cell stimulation (WholeSTIM) is consistent with those reported before [11, 15, 16]. Our results demonstrate that subcellular stimulation is sufficient to induce activity-dependent axon myelination. Stimulation of the somatic compartment (SomaSTIM) activated cell bodies and proximal axons and resulted in the anterograde signal propagation to the distal axons in the axonal compartment that were not directly stimulated. This stimulation was sufficient to induce the same effect as the whole cell stimulation. Similarly, when the electrodes were located in the axonal compartment (AxonSTIM), we observed an increase of the OPCs differentiation and myelin sheath formation on the same level as after WholeSTIM and SomaSTIM. Two plausible mechanisms can explain this observation: (1) activated axons propagated signal to the cell bodies and evoked global response; (2) local axonal activity induction is sufficient to induce activity-dependent myelination. Furthermore, in this mode, both distal axons and oligodendrocytes were exposed to the electric field. Recent studies show that OPCs can sense and migrate in the stable, small electric fields [27, 28]. Therefore, it cannot be excluded that OPCs directly responded to the stimulation. Although these questions are out of the scope of this study, our experimental platform offers multiple advantageous for such an investigation.

The effects of ESTIM are in agreement with the recent reports from *in vivo* studies showing that neural activity supports and stabilizes myelin sheath formation by oligodendrocytes [10, 12, 29]. As the induction of signal activity in a brain *in vivo* usually does not facilitate classification of the stimulation to whole cell, axons or soma, it is plausible to assume that the observed effects on myelination are an outcome of all those modes of treatment. Therefore it is important to understand if there are differences in the effects of the focal *vs.* global stimulation. Our input restriction assay facilitated testing this idea and demonstrated that focal axonal and somatic stimulations are sufficient to evoke OPCs differentiation into OLs and myelin sheath formation. These results not only provide

mechanistic insight into the activity-dependent myelination but also may be useful for designing therapeutic strategies for de-myelination diseases.

Conclusions

It has become abundantly clear that the role of myelination in the central nervous system expands beyond expediting electrical signal propagation. One of the key challenges in the emerging field of myelin plasticity is to link changes in neuron activity with specific myelination profiles [2]. Answering this and other questions require new tools. In this study, we present a compartmentalized neuron/oligodendrocyte co-culture device integrated with electrical stimulation system that allows applying whole cell and spatially restricted cell activity induction. This platform offers multiple advantages for studying activity-induced myelination, including: (1) ease of manipulation and integration with standard optical and molecular biology techniques; (2) restriction of oligodendrocyte interaction to distal axons to better replicate the *in vivo* scenario; and finally, (3) spatial restriction of the electrical stimulation input to a chosen subcellular region of neurons. There is no surprise that the popularity of the compartmentalized culture systems for neuronal studies has been increasing for the last decade. Commercially available systems can be easily integrated with the electrical stimulation. However, our simulations of the electric field emphasize that electrode locations have to be carefully designed. Using too sparsely located electrodes in somatic and axonal compartment may result in an uneven electric field, and cause three different spatial modes of neuron activity induction (whole cell, somatic and axonal) within one culture. Finally, we demonstrate that restricting electrical stimulation to distal axons or cell bodies is sufficient to induce activity-dependent axon myelination on the same level as whole cell electrical stimulation. This intriguing observation has to be further investigated.

Competing Interests

The authors declare that there is no conflict of interest regarding the publication of this paper

Acknowledgments

References

1. de Hoz, L. and M. Simons, *The emerging functions of oligodendrocytes in regulating neuronal network behaviour.* Bioessays, 2015. **37**(1): p. 60-9.

2. Chang, K.J., S.A. Redmond, and J.R. Chan, *Remodeling myelination: implications for mechanisms of neural plasticity.* Nat Neurosci, 2016. **19**(2): p. 190-7.

3. Makinodan, M., et al., *A critical period for social experience-dependent oligodendrocyte maturation and myelination.* Science, 2012. **337**(6100): p. 1357-60.

4. Liu, J., et al., *Impaired adult myelination in the prefrontal cortex of socially isolated mice.* Nat Neurosci, 2012. **15**(12): p. 1621-3.

5. McKenzie, I.A., et al., *Motor skill learning requires active central myelination.* Science, 2014. **346**(6207): p. 318-22.

6. Waxman, S.G., *Determinants of conduction velocity in myelinated nerve fibers.* Muscle Nerve, 1980. **3**(2): p. 141-50.

7. Rosenberg, S.S., et al., *The geometric and spatial constraints of the microenvironment induce oligodendrocyte differentiation.* Proc Natl Acad Sci U S A, 2008. **105**(38): p. 14662-7.

8. Lee, S., et al., *A culture system to study oligodendrocyte myelination processes using engineered nanofibers.* Nat Methods, 2012. **9**(9): p. 917-22.

9. Li, Q., et al., *Electrical stimulation of the medullary pyramid promotes proliferation and differentiation of oligodendrocyte progenitor cells in the corticospinal tract of the adult rat.* Neurosci Lett, 2010. **479**(2): p. 128-33.

10. Hines, J.H., et al., *Neuronal activity biases axon selection for myelination in vivo.* Nat Neurosci, 2015. **18**(5): p. 683-9.

11. Malone, M., et al., *Neuronal activity promotes myelination via a cAMP pathway.* Glia, 2013. **61**(6): p. 843-54.

12. Gibson, E.M., et al., *Neuronal activity promotes oligodendrogenesis and adaptive myelination in the mammalian brain.* Science, 2014. **344**(6183): p. 1252304.

13. Park, J., et al., *Microfluidic compartmentalized co-culture platform for CNS axon myelination research.* Biomed Microdevices, 2009. **11**(6): p. 1145-53.

14. Kerman, B.E., et al., *In vitro myelin formation using embryonic stem cells.* Development, 2015. **142**(12): p. 2213-25.

15. Ishibashi, T., et al., *Astrocytes promote myelination in response to electrical impulses.* Neuron, 2006. **49**(6): p. 823-32.

16. Yang, I.H., et al., *Axon myelination and electrical stimulation in a microfluidic, compartmentalized cell culture platform.* Neuromolecular Med, 2012. **14**(2): p. 112-8.

17. Park, H.S., et al., *Neuromuscular junction in a microfluidic device.* Conf Proc IEEE Eng Med Biol Soc, 2013. **2013**: p. 2833-5.

18. Yang, I.H., et al., *Compartmentalized microfluidic culture platform to study mechanism of paclitaxel-induced axonal degeneration.* Exp Neurol, 2009. **218**(1): p. 124-8.

19. Gadani, D.H., et al., *Effect of salinity on the dielectric properties of water.* Indian Journal of Pure & Applied Physics IJPAP, 2012. **50**(6): p. 405-410.

20. G., M.C. and M.A. A., *Dielectric Constant of Water from 0 0 to 1000 C.* Journal of Research of the National Bureau of Standards 1956. **56**(1).

21. ACM, K., *The Polymer Data Handbook.* 1999: Oxford University Press.

22. Radman, T., et al., *Role of cortical cell type and morphology in subthreshold and suprathreshold uniform electric field stimulation in vitro.* Brain Stimul, 2009. **2**(4): p. 215-28, 228 e1-3.

23. RD, F., et al., *Chronic electrical stimulation of multicompartment cell cultures.*, in *Practical Electrophysiological Methods.*, G. R, Editor. 1992, Wiley Press: New York. p. 67–76.

24. Charvet, G., et al., *A modular 256-channel micro electrode array platform for in vitro and in vivo neural stimulation and recording: BioMEA.* Conf Proc IEEE Eng Med Biol Soc, 2010. **2010**: p. 1804-7.

25. Stevens, B., et al., *Adenosine: a neuron-glial transmitter promoting myelination in the CNS in response to action potentials.* Neuron, 2002. **36**(5): p. 855-68.

26. Baumann, N. and D. Pham-Dinh, *Biology of oligodendrocyte and myelin in the mammalian central nervous system.* Physiol Rev, 2001. **81**(2): p. 871-927.

27. Li, Y., et al., *ARP2/3 complex is required for directional migration of neural stem cell-derived oligodendrocyte precursors in electric fields.* Stem Cell Res Ther, 2015. **6**: p. 41.

28. Li, Y., X. Wang, and L. Yao, *Directional migration and transcriptional analysis of oligodendrocyte precursors subjected to stimulation of electrical signal.* Am J Physiol Cell Physiol, 2015. **309**(8): p. C532-40.

29. Mensch, S., et al., *Synaptic vesicle release regulates myelin sheath number of individual oligodendrocytes in vivo.* Nat Neurosci, 2015. **18**(5): p. 628-30.